

# Large-scale brain network connectivity under anxiety induced by naturalistic story listening

Nathan Chang<sup>1</sup>, Il-Joo Cho<sup>2</sup>

<sup>1</sup> Branham High School, San Jose, CA, USA

<sup>2</sup> Department of Biomedical Sciences, College of Medicine, Korea University, Seoul, Korea

## SUMMARY

The triple network model, encompassing the salience network (SN), default mode network (DMN), and central executive network (CEN) in the brain, provides a framework for understanding how anxiety influences brain activity. Dysfunction in these networks is linked to anxiety disorders, suggesting their interaction is key to the condition. We hypothesized that anxiety from naturalistic story listening alters functional connectivity within this model. Specifically, we predict that at the story's peak tension, the anxiety-induced group will show significantly different connectivity—particularly increased network density—between the SN, DMN, and CEN compared to a control group. This naturalistic approach mimics real-life anxiety, unlike traditional artificial stressors. We tested this hypothesis using a previously published functional magnetic resonance imaging (fMRI) dataset where anxiety was manipulated during story listening. The story, *Pretty Mouth and Green My Eyes*, was narrated to two different groups; one anxiety-inducing (experimental) and one neutral (control). Consistent with this prediction, the network density (i.e., the degree to which different brain regions communicate), was significantly greater in the experimental group compared to the control group. In particular, the CEN serves as a bridge tightly connecting the DMN and SN, which may be interpreted as empathy and emotion coming together under focused attention when experiencing tension. Our findings demonstrate that anxiety and tension during reading significantly alter the functional connectivity of the SN, DMN, and CEN. This research provides a possibility for creating accurate diagnostic tools and personalized treatments for anxiety disorders by comparing connectivity patterns of those without and with anxiety disorders.

## INTRODUCTION

Anxiety, a complex emotional state, is a prevalent mental health concern that significantly impacts individuals' well-being and daily functioning (1, 2). Understanding the neural mechanisms underlying anxiety is crucial for developing effective diagnostic tools and personalized treatments for anxiety disorders, including post-traumatic stress disorder (PTSD) and obsessive-compulsive disorder (OCD) (1, 2). The human brain is an intricate and highly sophisticated organ, responsible for interpreting senses, initiating body movement and behavior, and intelligence (1). It functions by using neurons that communicate with each other by transmitting electrochemical signals (1). Functional magnetic

resonance imaging (fMRI) allows us to observe activity in specific brain regions during certain tasks (1). When a particular brain region is active, it consumes more oxygen, resulting in enhanced blood flow that is captured by the blood-oxygen-level dependent (BOLD) signal, an indirect measure of neural activity (1).

The fMRI literature has identified distinct brain regions that show coordinated activity patterns (functional connectivity) during different psychological states, suggesting they form large-scale functional networks (1, 4, 7). The triple network model is one prominent example, consisting of key interacting networks relevant to understanding mental and neurological disorders (1). This model consists of the salience network (SN), the default mode network (DMN), and the central executive network (CEN) (1) (Figure 1).

The core components of the SN, being the anterior insula and the anterior cingulate cortex, along with other structures such as the amygdala and thalamus, are crucial for various functions such as interoception, emotions, empathy, cognitive control, and information processing (3). A key function of the SN is its role in regulating the activity of the DMN and the CEN by switching the brain's activity between these two networks (4, 5).

The DMN is a large-scale brain network that functions during a resting state and introspective activity, such as mind-wandering (6). In a classic study, researchers used quantitative metabolic and circulatory measurements to discover that there was a baseline state in the brain (7). They identified specific brain regions including the posterior cingulate, precuneus, and medial prefrontal cortex that consistently decrease their activity during various tasks (7). Other functional implications of the DMN include its lesser-known roles in the abstraction and granularity of emotions (7). For example, the DMN plays a role in creating discrete emotions like anger, fear and disgust by abstracting them from concrete features (2).

The CEN, referred to as the frontoparietal network, is essential for tasks requiring prolonged concentration, advanced problem-solving abilities, and the regulation of working memory (1). Anatomically, this network includes the posterior parietal cortex and the dorsolateral prefrontal cortices (6). It is involved in goal-oriented behavior and is generally thought of as the opposite of the DMN. The CEN serves as a versatile hub among brain networks, enabling adaptable coordination of cognitive control by interacting with the DMN, visual network, auditory network, and others.

These networks are known to be affected by anxiety. Excessive activity of the anterior insula within the SN has been linked to anxiety disorders (2). Similarly, hyperactivity in

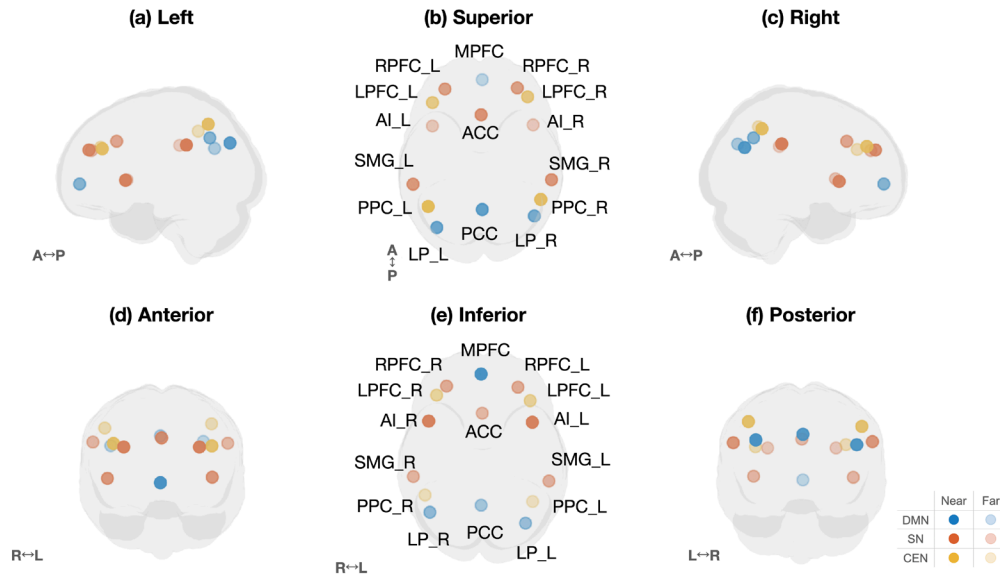


**Figure 1. Three-dimensional brain renderings with the spatial locations of nodes within the triple network model.** The anatomical distribution of the networks is shown from six different angles: (A) left, (B) superior, (C) right, (D) anterior, (E) inferior, and (F) posterior. Nodes are color-coded to represent the salience network (SN; red), default mode network (DMN; blue), and central executive network (CEN; yellow). Color densities represent depth, with brighter colors indicating regions closer to the human observer. Abbreviations: MPFC, medial prefrontal cortex; LP, lateral parietal lobe; PCC, posterior cingulate cortex; ACC, anterior cingulate cortex; AI, anterior insula; RPFC, rostral prefrontal cortex; SMG, supramarginal gyrus; LPFC, lateral prefrontal cortex; PPC, posterior parietal cortex; L, left; R, right; see Table 1 for the full ROI names and MNI coordinates.

the amygdala is frequently observed across various anxiety disorders (1). Anxiety also affects the DMN with anterior DMN activity increasing with higher anxiety while posterior DMN activity decreases (8). The CEN is also affected, with the superior frontal gyrus showing decreased positive connections in those with generalized anxiety disorder (9).

To appreciate the value of our naturalistic approach, it is helpful to consider how anxiety has typically been studied. Historically, anxiety has been examined by exposing mice to

stressful situations or having human subjects inhale carbon dioxide (10, 11). Other methods include mock interviews with mental arithmetic tests or submerging limbs in ice water (12, 13). Although these artificial stressors are effective in eliciting anxiety, they are a stark contrast to the real-life experiences of anxiety.

Our study takes a unique approach by examining brain connectivity during the reading of an anxiety-provoking short story (14). This naturalistic setting mimics the way anxiety can

Network	Anatomical Region		x	y	z
DMN	Medial Prefrontal Cortex	MPFC	1	55	-3
	Lateral Parietal Lobe (left)	LP_L	-39	-77	33
	Lateral Parietal Lobe (right)	LP_R	47	-67	29
	Posterior Cingulate Cortex	PCC	1	-61	38
SN	Anterior Cingulate Cortex	ACC	0	22	35
	Anterior Insula (left)	AI_L	-44	13	1
	Anterior Insula (right)	AI_R	47	14	0
	Rostral Prefrontal Cortex (left)	RPFC_L	-32	45	27
	Rostral Prefrontal Cortex (right)	RPFC_R	32	46	27
	Supramarginal Gyrus (left)	SMG_L	-60	-39	31
	Supramarginal Gyrus (right)	SMG_R	62	-35	32
CEN	Lateral Prefrontal Cortex (left)	LPFC_L	-43	33	28
	Lateral Prefrontal Cortex (right)	LPFC_R	41	38	30
	Posterior Parietal Cortex (left)	PPC_L	-46	-58	49
	Posterior Parietal Cortex (right)	PPC_R	52	-52	45

**Table 1. Regions of interest (ROI) within the Default Mode Network (DMN), Salience Network (SN), and Central Executive Network (CEN) used in this study.** Coordinates are provided in Montreal Neurological Institute (MNI) space. ROIs were defined based on coordinates from the CONN toolbox network atlas and extracted as spherical regions with a 10-voxel radius.

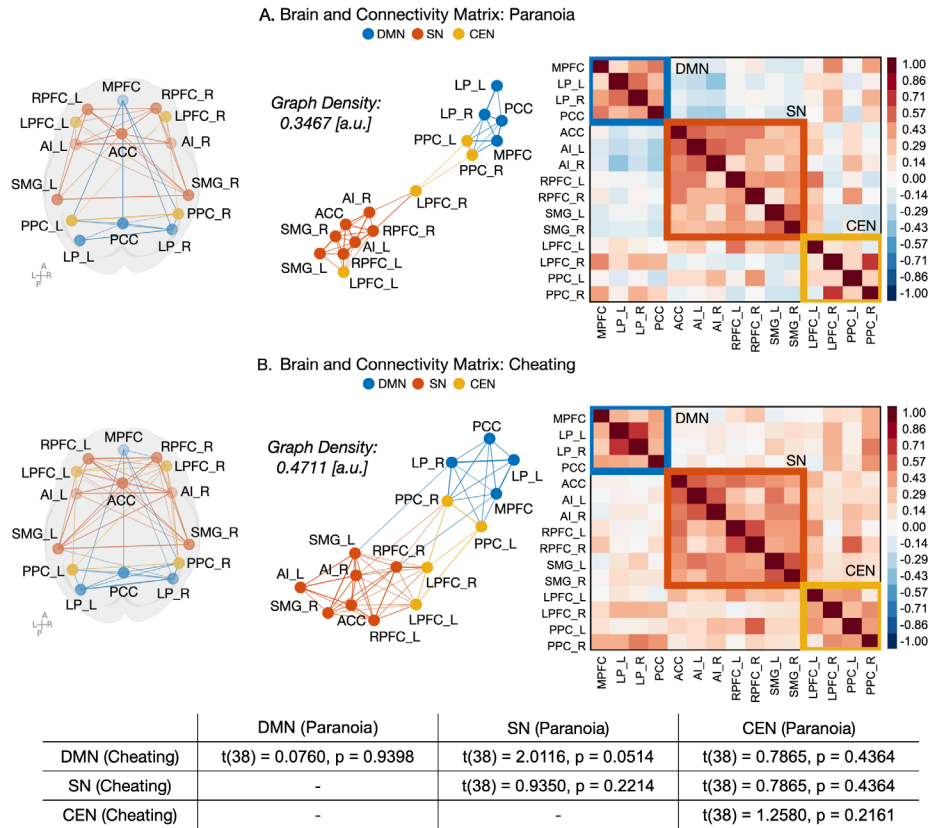


**Figure 2. Brain connectivity at the peak tension point in the story.** Functional connectivity is shown for (A) the control ('paranoia') group and (B) the cheating group. Nodes represent regions of interest (ROIs) within the SN, DMN, and CEN. Edges represent significant functional connections (threshold set at  $r > 0.2$ ). The cheating group shows increased network density, particularly between the DMN and SN, with the CEN acting as a bridge. Statistical analysis revealed a significant difference in overall network density between groups ( $p = 0.0490$ ). Direct comparisons of correlation coefficients showed no significant differences in inter- or within-network connectivity ( $p > 0.05$  for all). The table beneath the figure reports between-group comparisons of connectivity strength for each within-network and between-network pairing among the DMN, SN, and CEN, none of which were significant. Sample size:  $n = 20$  per group. Abbreviations defined in Table 1.

arise in everyday situations. Based on the findings that anxiety affects components of the triple network, we hypothesized that anxiety is represented by altered functional connectivity patterns within and between the SN, DMN, and CEN. We tested this by using public fMRI datasets to measure how connectivity within the triple network model changes during moments of tension and release. By comparing responses between individuals who felt anxious while listening to the story and those who did not, we identified brain network signatures that could serve as potential markers for anxiety disorders and help in the development of a diagnostic tool and personalized treatments.

## RESULTS

This study analyzed a publicly available fMRI dataset where participants listened to a short story ("Pretty Mouth and Green My Eyes") after receiving one of two narrative contexts (14). One context aimed to induce anxiety and tension related to potential infidelity (the 'cheating' group,  $n=20$ ), while the other served as a control (the 'control' group,  $n=20$ ). We investigated differences in functional connectivity within the triple network model between these groups, particularly

during moments of high narrative tension. The network density computed from the functional connectivity patterns at the peak tension time point was 0.3467 a.u. in the control group and 0.4711 a.u. in the cheating group (Figure 2). This difference was found to be statistically significant ( $p=0.0490$ ). These results indicate that anxiety and tension in the story alter the properties of the triple network.

As visualized in the connectivity graphs, we observed several patterns in the connectivity of nodes (Figure 2). The DMN and the SN were positioned on opposite sides of the graph, with the CEN positioned centrally, connecting the two other networks. In the control case, the right lateral prefrontal cortex in the CEN was centrally located, working like a hub for the connection with the SN and the two posterior parietal cortices. The two posterior parietal cortices were connected to the DMN nodes, linking the SN to other regions of interest. Notably, the right lateral prefrontal cortices communicated exclusively with the SN and CEN members, whereas the left posterior parietal cortex interacted solely with the DMN and CEN members. Additionally, the right posterior parietal cortex was unique in its correlation with both the SN and DMN, making it the only node to correlate with all three networks.

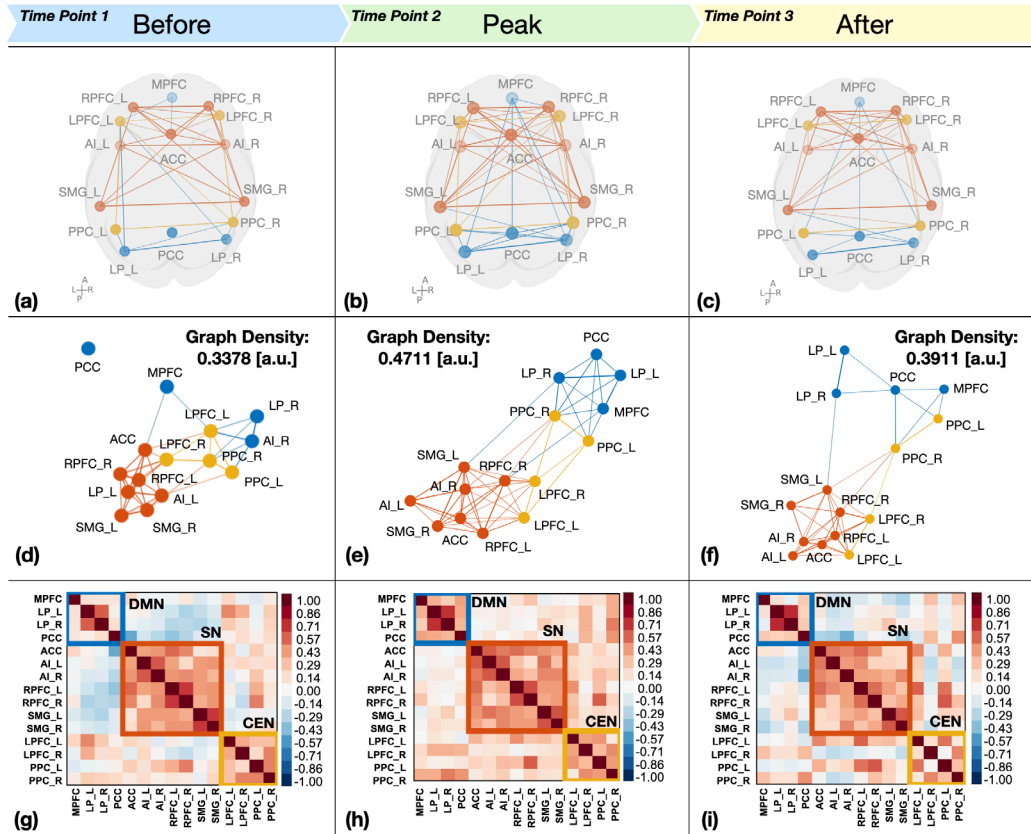


**Figure 3. Connectivity graphs for the cheating group at three time points: before peak tension (Time Point 1), at peak tension (Time Point 2), and after tension release (Time Point 3) (n = 20).** Sub-figures (A-C) show the circular functional connectivity graphs for Time Points 1, 2, and 3, respectively; sub-figures (D-F) show the network layout graphs for Time Points 1, 2, 3, respectively; and sub-figures (G-I) show the connectivity matrices for Time Points 1, 2, and 3, respectively. Nodes represent ROIs within the Salience Network (SN), Default Mode Network (DMN), and Central Executive Network (CEN), and edges represent significant functional connections (threshold set at  $r > 0.2$ ). Graph density increased from 0.3378 in sub-figure (D) before tension to 0.4711 in sub-figure (E) at peak tension and then decreased to 0.3911 in sub-figure (F) after tension release. The increased clustering of DMN nodes at peak tension suggests heightened internal communication during anxiety. Abbreviations defined in Table 1.

Aside from graph density, a direct comparison between the correlation coefficients in the correlation matrices was performed to evaluate the strength of connectivity both within and between networks (Figure 2). The averaged  $r$  values were compared between the cheating and the control groups using a  $t$ -test.

The correlation coefficients between the nodes in the CEN and SN showed no significant difference in connectivity strength between the groups ( $t(38) = 1.7224, p = 0.0931$ ) (Figure 2). Similarly, connectivity strength between the CEN and DMN did not differ significantly between the groups ( $t(38) = 0.7865, p = 0.4364$ ) (Figure 2). The comparison between the SN and DMN also showed no significant difference in connectivity strength ( $t(38) = 2.0116, p = 0.0514$ ), although it was trending in that direction (Figure 2). Connectivity within each of the three networks also did not differ significantly between the two groups (DMN:  $t(38) = 0.0760, p = 0.9398$ ; SN:  $t(38) = 0.9350, p = 0.2214$ ; CEN:  $t(38) = 1.2580, p = 0.2161$ ) (Figure 2). Together, these results suggest that the group difference at peak tension was reflected in overall network density rather than in specific pairwise or within-network connectivity strengths.

In addition to comparing network connectivity between groups at the peak of tension, we examined how connectivity patterns in the cheating group evolved across time points corresponding to tension buildup, peak tension, and post-tension release (Figure 3). Overall network density dynamically followed the narrative arc, increasing from 0.3378 before the tension peak (Time Point 1) to a maximum of 0.4711 at the peak (Time Point 2), before decreasing to 0.3911 after the tension release (Time Point 3).

Although at the conventional alpha level of 0.05 ( $p > 0.05$  for the other time point comparisons), the trend observed between the 'before peak' and 'peak' time points ( $p = 0.0575$ ) suggests potential dynamic alterations in functional connectivity patterns occur over time as participants in the cheating group experience the buildup and resolution of tension in the story.

## DISCUSSION

This study investigated how anxiety induced by naturalistic story listening affects functional connectivity within the triple network model, hypothesizing that anxiety would alter connectivity patterns within and between the salience

network, default mode network, and central executive network. Consistent with our hypothesis, we found significantly higher overall network density in participants presumed to be experiencing anxiety (the ‘cheating’ group) compared to the control group during the story’s peak tension. This increased density suggests heightened communication and integration across the SN, DMN, and CEN under anxiety. Furthermore, our analysis revealed dynamic changes in connectivity corresponding to the narrative tension arc and highlighted a potential bridging role for the CEN between the SN and DMN during peak anxiety.

These findings provide empirical support for the idea that an anxious state modulates large-scale network interactions. The greater network density observed in the cheating group likely reflects increased communication demands as the brain processes the heightened emotional salience and tension inherent in the anxiety-inducing narrative context. The SN is known to be active in detecting and orienting attention to salient stimuli (3), the DMN is involved in emotional regulation and self-reflection (6, 7), and the CEN in this case may have worked as a hub for effective communication (1). The resulting increase in collaboration across networks supports our prediction that anxiety alters their functional connectivity patterns.

We also observed trends throughout the tension buildup, peak tension, and tension release. After tension release, decreased connectivity was observed between the three networks. The DMN’s medial prefrontal cortex communicated with the SN before and at peak tension, but greatly decreased communication with the SN after tension release. This might be related to the medial prefrontal cortex’s function in processing social information, as well as in self-reflection and personal perception (15, 16). Therefore, after the bulk of emotional processing is done, the communication with the SN might decrease as the need for emotional regulation and processing diminishes.

The patterns we observed based on the triple network model may have implications for future research in anxiety disorders. Dysfunctions and anomalies across these networks have been associated with many clinical symptoms (1). For example, an overactive DMN may contribute to increased self-referential thought in depression and PTSD and altered DMN structure is linked to autism spectrum disorder (17). Impairments in the SN are believed to contribute to conditions like schizophrenia and ADHD (18–21). Likewise, overactivity in the CEN is thought to lead to obsessive-compulsive disorder, while weakened connections between the amygdala and the dorsolateral prefrontal cortex (dlPFC) are known to relate to anxiety disorder (22, 23). Our finding that acute anxiety heightens connectivity between these networks may provide a notable feature for studying these clinical disorders.

One limitation of the current study is that our interpretations rely on the assumption that the cheating group experienced more anxiety and tension than the control group. The original study only compared similarities and differences between the two groups and did not discuss the data in the context of tension and anxiety (14). Thus, there was no objective measure in the dataset indicating that the cheating group experienced more anxiety. Nevertheless, the observed differences in brain network connectivity between the groups

strongly suggest that the narrative context successfully affected the participants’ psychological state. This is particularly supported by the significantly higher network density and distinct interaction patterns involving the CEN in the cheating group at peak tension.

The goal of this study was to explore how anxiety and tension affect connectivity patterns within the triple network model during naturalistic story listening. Our results demonstrated increased functional connectivity between nodes of the DMN, SN, and CEN, when participants experienced anxiety due to heightened tension in the story. Characterizing brain connectivity patterns under anxiety may help create more accurate diagnoses and personalized treatment for mental disorders.

## MATERIALS AND METHODS

### Procedures

This study performed an original analysis of the publicly available dataset “Pretty Mouth and Green My Eyes,” which comprised 40 subjects categorized into two groups: cheating and control (14). These subjects listened to an adapted version of the short story “Pretty Mouth and Green My Eyes” by J. D. Salinger (14). The adapted version included some text that was not in the main story and was also shorter. The audio was 11 min and 32 seconds long, including 18 seconds of neutral music followed by 3 seconds of silence. This was then followed by an additional 15 seconds of silence. The reading was recorded by a professional actor. The story is about Arthur and Lee, two friends, having a phone conversation. Arthur is worried after losing his wife at a party and is calling Lee for support. Lee is at home with a woman by his side, though it is uncertain if she may or may not be Arthur’s wife. The control group was given the context that Arthur’s wife is not cheating on him (that is, the woman with Lee is not Arthur’s wife), while the cheating group was given the context that Arthur’s wife is cheating on him (that is, the woman with Lee is Arthur’s wife). These contexts made the story more tense and anxious for the cheating group. After obtaining the fMRI scan, the subjects were assessed using a questionnaire to determine comprehension.

### fMRI Data Acquisition

The raw data were originally acquired as described by Yeshurun et al. (14). Briefly, subjects underwent 3T MRI scans using a full-body scanner with foam padding to minimize head movement. MRI-compatible earbuds delivered the audio stimuli, and noise-canceling headphones were used for auditory isolation. Functional MRI data were acquired using a 3T Siemens Skyra full-body MRI scanner with a 12-channel head coil. The T2\*-weighted echo-planar imaging pulse sequence parameters included a repetition time (TR) of 1,500 ms, echo time (TE) of 28 ms, and a flip angle of 64°. Each volume comprised 27 interleaved slices of 4-mm thickness without a gap, with an in-plane resolution of 3 × 3 mm<sup>2</sup> and a field of view of 192 × 192 mm<sup>2</sup>.

### Preprocessing and Denoising of fMRI Data

For this study, we conducted all preprocessing, denoising, and first-level connectivity analyses using the CONN toolbox running in MATLAB (24). The raw functional data underwent

the default preprocessing pipeline within CONN, including realignment, slice-timing correction, outlier detection (using ART), segmentation, normalization to MNI space, and smoothing, using the toolbox's default parameters as detailed in the CONN documentation and boilerplate text (25). Denoising was performed using CONN's default pipeline (CompCor strategy).

### Regions of Interest (ROI)

Specific regions of interest within the triple network model encompassing the DMN, the SN, and the Fronto-Parietal Network were defined. These ROIs were determined by extracting spherical regions with a 10-voxel radius around peak coordinates provided by the CONN toolbox. These spherical ROIs ensure there is comprehensive coverage of the relevant brain areas.

### Time Points of Interest

To examine the effect of tension and anxiety on the triple network model, we specified excerpts from the adapted "Pretty Mouth and Green My Eyes" audio. One such portion was Lee's sudden desire to visit Arthur during their phone call. The time points used for the phone call were 288–305 TRs (432.0–457.5 sec).

### Computation of Functional Connectivity and Graph Theory

Functional connectivity was assessed by extracting spherical ROIs and computing the average BOLD signal within these ROIs. The correlations between BOLD signals across these ROIs were then calculated, resulting in a correlation matrix for each subject.

Pairwise correlations between all the ROIs represented connectivity between network nodes, and a threshold of  $r = 0.2$  was used to remove weak or negative connectivity. The correlation matrix was computed separately for the two groups. We then calculated the overall network densities for each of the two graphs, which measures the proportion of connections relative to all possible connections. The network densities and individual node connectivity were then compared between the two groups.

### Statistical Analysis

To determine if the observed difference in overall network density was statistically significant, a non-parametric permutation test was employed. The group labels (cheating vs. control) were randomly shuffled 100,000 times, and the difference in network density was recalculated for each permutation to build a null distribution.

To compare the strength of connectivity, independent samples t-tests were used to compare the average correlation coefficients between the cheating and control groups. The threshold for statistical significance was set at  $p < 0.05$  for all tests.

### ACKNOWLEDGMENTS

We would like to extend our heartfelt thanks to Dr. Joonkoo Park for his invaluable help during this research. His patience and willingness to provide guidance when needed made a significant difference. We truly appreciate his support and the

impact it had on the completion of this project.

**Received:** September 28, 2024

**Accepted:** May 1, 2025

**Published:** June 03, 2026

### REFERENCES

- Menon, Vinod. "Large-Scale Brain Networks and Psychopathology: A Unifying Triple Network Model." *Trends in Cognitive Sciences*, vol. 15, no. 10, Oct. 2011, pp. 483-506. <https://doi.org/10.1016/j.tics.2011.08.003>.
- Paulus, Martin P., and Murray B. Stein. "An Insular View of Anxiety." *Biological Psychiatry*, vol. 60, no. 4, 2006, pp. 383-87. <https://doi.org/10.1016/j.biopsych.2006.03.042>.
- Seeley, William W. "The Salience Network: A Neural System for Perceiving and Responding to Homeostatic Demands." *The Journal of Neuroscience*, vol. 39, no. 50, 11 Dec. 2019, pp. 9878-80. <https://doi.org/10.1523/JNEUROSCI.1138-17.2019>.
- Goulden, Nia, et al. "The Salience Network Is Responsible for Switching between the Default Mode Network and the Central Executive Network: Replication from DCM." *NeuroImage*, vol. 99, 2014, pp. 180-90. <https://doi.org/10.1016/j.neuroimage.2014.05.052>.
- Sridharan, Devarajan, et al. "A Critical Role for the Right Fronto-Insular Cortex in Switching between Central-Executive and Default-Mode Networks." *Proceedings of the National Academy of Sciences of the United States of America*, vol. 105, no. 34, 2008, pp. 12569-74. <https://doi.org/10.1073/pnas.0800005105>.
- Buckner, Randy L. "The Cerebellum and Cognitive Function: 25 Years of Insight from Anatomy and Neuroimaging." *Neuron*, vol. 80, no. 3, 2013, pp. 807-15. <https://doi.org/10.1016/j.neuron.2013.10.044>.
- Satpute, Ajay B., et al. "The Default Mode Network's Role in Discrete Emotion." *Trends in Cognitive Sciences*, vol. 23, no. 10, 2019, pp. 851-64. <https://doi.org/10.1016/j.tics.2019.07.003>.
- Coutinho, Joana Fernandes, et al. "Default Mode Network Dissociation in Depressive and Anxiety States." *Brain Imaging and Behavior*, vol. 10, no. 1, 2016, pp. 147-57. <https://doi.org/10.1007/s11682-015-9375-7>.
- Li, Chunlin, et al. "Abnormal Spontaneous Brain Activity in Patients with Generalized Anxiety Disorder Revealed by Resting-State Functional MRI." *NeuroReport*, vol. 29, no. 5, 2018, pp. 397-401. <https://doi.org/10.1097/WNR.0000000000000982>.
- Perna, Giampaolo, et al. "Carbon Dioxide/Oxygen Challenge Test in Panic Disorder." *Psychiatry Research*, vol. 52, no. 2, May 1994, pp. 159-71. [https://doi.org/10.1016/0165-1781\(94\)90085-X](https://doi.org/10.1016/0165-1781(94)90085-X).
- Shilton, Alexandra L., et al. "The Maastricht Acute Stress Test (MAST): Physiological and Subjective Responses in Anticipation, and Post-Stress." *Frontiers in Psychology*, vol. 8, 2017, article 567. <https://doi.org/10.3389/fpsyg.2017.00567>.
- Hart, Peter C., et al. "Experimental Models of Anxiety for Drug Discovery and Brain Research." *Methods in Molecular Biology*, edited by Gabriele Proetzel and Michael V. Wiles, vol. 602, Humana Press, 2010, pp.

- 299-321. [https://doi.org/10.1007/978-1-60761-058-8\\_18](https://doi.org/10.1007/978-1-60761-058-8_18).
13. Allen, Andrew P., et al. "The Trier Social Stress Test: Principles and Practice." *Neurobiology of Stress*, vol. 6, 2017, pp. 113-26. <https://doi.org/10.1016/j.ynstr.2016.11.001>.
14. Yeshurun, Yaara, et al. "Same Story, Different Story." *Psychological Science*, vol. 28, no. 3, Mar. 2017, pp. 307-19. <https://doi.org/10.1177/0956797616682029>.
15. Amodio, David M., and Chris D. Frith. "Meeting of Minds: The Medial Frontal Cortex and Social Cognition." *Nature Reviews Neuroscience*, vol. 7, no. 4, 2006, pp. 268-77. <https://doi.org/10.1038/nrn1884>.
16. Frith, Chris D., and Uta Frith. "The Neural Basis of Mentalizing." *Neuron*, vol. 50, no. 4, 2006, pp. 531-34. <https://doi.org/10.1016/j.neuron.2006.05.001>.
17. Padmanabhan, Aarthi, et al. "The Default Mode Network in Autism." *Biological Psychiatry: Cognitive Neuroscience and Neuroimaging*, vol. 2, no. 6, Sept. 2017, pp. 476-86. <https://doi.org/10.1016/j.bpsc.2017.04.004>.
18. Uddin, Lucina Q. *The Salience Network of the Human Brain*. Academic Press, 2017.
19. Palaniyappan, Lokesh, et al. "Reality Distortion Is Related to the Structure of the Salience Network in Schizophrenia." *Psychological Medicine*, vol. 41, no. 8, 2011, pp. 1701-08. <https://doi.org/10.1017/S0033291710002205>.
20. Chiong, Winston, et al. "The Salience Network Causally Influences Default Mode Network Activity during Moral Reasoning." *Brain*, vol. 136, no. 6, 2013, pp. 1929-41. <https://doi.org/10.1093/brain/awt066>.
21. Castellanos, F. Xavier, et al. "Cingulate-Precuneus Interactions: A New Locus of Dysfunction in Adult Attention-Deficit/Hyperactivity Disorder." *Biological Psychiatry*, vol. 63, no. 3, 2008, pp. 332-37. <https://doi.org/10.1016/j.biopsych.2007.06.025>.
22. Chen, Yunhui, et al. "Altered Resting-State Functional Organization within the Central Executive Network in Obsessive-Compulsive Disorder." *Psychiatry and Clinical Neurosciences*, vol. 70, no. 10, 2016, pp. 448-56. <https://doi.org/10.1111/pcn.12419>.
23. Kolesar, Tiffany A., et al. "Systematic Review and Meta-Analyses of Neural Structural and Functional Differences in Generalized Anxiety Disorder and Healthy Controls Using Magnetic Resonance Imaging." *NeuroImage: Clinical*, vol. 24, 2019, article 102016. <https://doi.org/10.1016/j.nicl.2019.102016>.
24. Whitfield-Gabrieli, Susan, and Alfonso Nieto-Castanon. "CONN: A Functional Connectivity Toolbox for Correlated and Anticorrelated Brain Networks." *Brain Connectivity*, vol. 2, no. 3, 2012, pp. 125-41. <https://doi.org/10.1089/brain.2012.0073>.
25. Nieto-Castanon, Alfonso. *Handbook of Functional Connectivity Magnetic Resonance Imaging Methods in CONN*. Hilbert Press, 2020. <https://doi.org/10.56441/hilbertpress.2207.6598>.

provided that you credit the original author and source, include a link to the license, indicate any changes that were made, and make no representation that JEI or the original author(s) endorse you or your use of the work. The full details of the license are available at <https://creativecommons.org/licenses/by-nc-nd/4.0/deed.en>.

**Copyright:** © 2026 Chang and Cho. All JEI articles are distributed under the Creative Commons Attribution Noncommercial No Derivatives 4.0 International License. This means that you are free to share, copy, redistribute, remix, transform, or build upon the material for any purpose,